Research Square

Preprints are preliminary reports that have not undergone peer review.
They should not be considered conclusive, used to inform clinical practice,
or referenced by the media as validated information.

No solid evidence for an inner core on Mars

Marjolein Visser
ETH Zurich
Federico Munch
federico.munch@eaps.ethz.ch

ETH Zurich https://orcid.org/0000-0002-9472-168X
Amir Khan
amir.khan@eaps.ethz.ch

ETH Zurich
Daniel Andrew Frost
University of South Carolina
Domenico Giardini
ETH Zurich

Research Article

Keywords:

Posted Date: July 20th, 2026

DOI: https://doi.org/10.21203/rs.3.rs-10379955/v1

License: This work is licensed under a Creative Commons Attribution 4.0 International License.
Read Full License

Additional Declarations: The authors declare no competing interests.

No solid evidence for an inner core on Mars

M. Visser[1], F. D. Munch[1], A. Khan[2], D. A. Frost[3], D. Giardini[1]

[1]Institute of Geophysics, ETH Zurich, Zurich, Switzerland
[2]Institute of Geochemistry and Petrology, ETH Zurich, Zurich, Switzerland
[3]School of the Earth Ocean and Environment, University of South Carolina, Columbia, SC, USA

Key Points:

- We analysed InSight seismic data from Mars for potential inner-core signals.
- Coherent signals that could be attributed to e.g., inner-core reflections were identified for a range of different inner-core radii (200–300 and 500–600 km)
- This ambiguity implies that there is no solid evidence for an inner-core on Mars

Corresponding author: F. D. Munch, federico.munch@eaps.ethz.ch

Corresponding author: A. Khan, amir.khan@eaps.ethz.ch

Abstract

We searched the Mars InSight seismic data for signals that would indicate the presence of an inner core, such as the inner-core boundary-reflecting phase, PKiKP, and the bottom-side outer-core-reflection, PKIKKIKP. For this, we analysed the highest-quality events from the seismically most active region (Cerberus Fossae) detected on Mars. Using source-array methods, we compute vespagrams and associated F-vespagrams, wherein a strong energy peak at a specific time and horizontal slowness indicates a coherent seismic phase. We validated our method on body wave phases seen earlier by the InSight team, such as SS. Application to PKiKP and PKIKKIKP produces coherent signals for a range of candidate inner-core radii, specifically 200–300 km and 500–600 km for PKiKP and 100–600 km for PKIKKIKP. This suggests that the interpretation of inner-core seismic signals is not unique and, consequently, there is no definitive evidence confirming the existence of an inner core on Mars.

Plain Language Summary

Since NASA's InSight mission began recording marsquakes, major advances in our understanding Mars's interior have been made. Early studies suggested the planet has a large liquid metal core, but later evidence indicated that the core is likely smaller and denser than first thought, with a layer of molten rock lying above it. An important question is whether Mars, like Earth, also has a solid inner core. If confirmed, this would help better understand how Mars cooled over time and how it once generated a global magnetic field. To address the question of an inner core, we re-examined the same seismic data using methods that combine signals from multiple marsquakes to improve their clarity. We found that the signals previously interpreted as evidence for a 600 km inner core can also be explained by a wide range of smaller inner-core sizes. Because the data do not point to a single, unique solution, we conclude that there is currently no convincing seismic evidence that Mars has a solid inner core. More observations will be needed to determine whether Mars truly harbors an inner core.

1 Introduction

Since the arrival of InSight at Mars and initial analysis of the seismic data (Banerdt et al., 2020; Lognonné et al., 2023), the core of Mars has proved a bit of a conundrum. Early studies based mainly on events from Cerberus Fossae—a graben system located at an epicentral distance between 25–35° East of InSight—indicated a large (1830±40 km), low-density metal-rich liquid core (6–6.3 g/ccm) (Stähler et al., 2021; Durán et al., 2022; Irving et al., 2023), requiring in excess of 20 wt% light elements (chiefly S, C, O and H) that are possibly at odds with their cosmochemical availability (e.g., Khan et al., 2022). A far side meteoroid impact (Posiolova et al., 2022) has subsequently offered a partial solution to this problem in the form of diffracted P-waves (Durán et al., 2022) that appear to indicate a stratified core-mantle boundary region incorporating a lowermost fully molten mantle atop a smaller (1670±35 km), denser (6.5–6.7 g/ccm) liquid Fe-metal rich core rather than a large liquid core (Khan et al., 2023; Samuel et al., 2023), reducing the amount of light elements to 9–15 wt%.

A question that remained unaddressed, however, was that of an inner core. Although a solid inner core is not precluded, the predicted amount of light elements in combination with the physical conditions of the core (2000–3000 K and 19–40 GPa) would tend to argue in favour of a purely liquid core at present (e.g., Buono & Walker, 2011; Komabayashi et al., 2026). Coupled herewith is the nature of the seismic data from Mars. Most of the events emanating from Cerberus Fossae are small-magnitude events (2.5–4) (Brinkman et al., 2021; Jacob et al., 2022; Perrin et al., 2022; Stähler et al., 2022) that, apart from relatively clear direct P- and S-wave arrivals, are chiefly characterised by scattering coda,

which tends to obscure secondary arrivals, particularly small-amplitude seismic arrivals associated with the core.

In spite of these difficulties, Bi et al. (2025) have recently suggested evidence in favour of a solid inner core on Mars based on the alleged identification of PKiKP (reflection from the top of the inner core) and PKIKKIKP (reflection from the inside of the liquid outer core with inner-core traversal) from seismic events in and around Cerberus Fossae (Figure 1). From the two phases, Bi et al. (2025) infer a solid 600-km inner core. If true, the observation is of utmost significance given that a crystallising core is a window into the thermo-chemical conditions of Mars's deep interior and forms important anchoring points for understanding how the core evolved and possibly produced a dynamo that magnetised the Martian crust early on (e.g., Stevenson, 2001; Mittelholz et al., 2020; Yan et al., 2025).

Establishing the existence of a solid inner core beyond reasonable doubt is therefore of fundamental importance. To investigate this, we re-examined the InSight seismic data by focusing on the PKiKP phase. Unlike PKIKKIKP, whose travel time depends on poorly constrained inner-core P-wave velocities and thus introduces additional uncertainty, PKiKP provides the most direct test because its travel time is controlled by the relatively well-constrained properties of the mantle and core, leaving the inner-core radius as the only unknown parameter. If no robust PKiKP arrival can be identified, phases involving additional interactions with the inner core are unlikely to provide stronger or less ambiguous constraints, as will be demonstrated here. Thus, for completeness, we also examine the PKIKKIKP phase.

Relying on array analysis methods (e.g., Rost & Thomas, 2002; Thomas et al., 2025) to stack events and enhance signal-to-noise ratio (as also done by Bi et al., 2025), we found that PKiKP signals from a 600-km inner-core are not unique. Similar signals are also obtained for smaller inner-core radii (e.g., 200, 300 and 500 km) and, in the case of PKIKKIKP, for inner-core radii from 100 to 600 km. These results ultimately suggest that conclusive proof of a solid inner core on Mars is lacking.

2 Methodology

In cases of low signal-to-noise ratio (SNR), stacking of seismic traces can increase the prominence of the phase of interest by constructive interference of the coherent signal, and destructive interference of the incoherent noise (e.g., Rost & Thomas, 2002, 2009). This is typically applied at arrays of multiple, closely located seismometers. However, the principle of reciprocity allows swapping of the source and receiver, thus stacking of multiple sources at a single seismometer is also feasible for improving SNR (Niazi, 1969; Spudich & Bostwick, 1987; Scherbaum et al., 1991). Mars only has one seismometer, but multiple sources, thus we apply source stacking to the Marsquakes recorded at InSight.

We selected 23 marsquakes from the low-frequency family of events from the MQS catalog (InSight Marsquake Service, 2023), consisting of 10 quality A and 13 quality B events (compiled in Table S1)—the same events considered by Bi et al. (2025). These events represent the high-quality events from the Cerberus Fossae area—the most seismically prolific region detected on Mars—located about 30° due East of InSight (Perrin et al., 2022; Stähler et al., 2022) (Figure 1) and resulting in a reference epicentral distance of 31°. For each event, the deglitched waveforms are rotated into the radial-transverse-vertical (RTZ) system and filtered using: 1) a band-pass Butterworth filter between 0.2 and 0.9 Hz and 2) a time-domain polarisation filter that increases the signal-to-noise of the linearly polarised part of the signal that involves body wave phases (Montalbetti & Kanasewich, 1970). Acknowledging the differences in magnitude and distance of the Marsquakes used, we normalise each trace by its maximum within a window of ±100 s around the predicted time for the phase of interest.

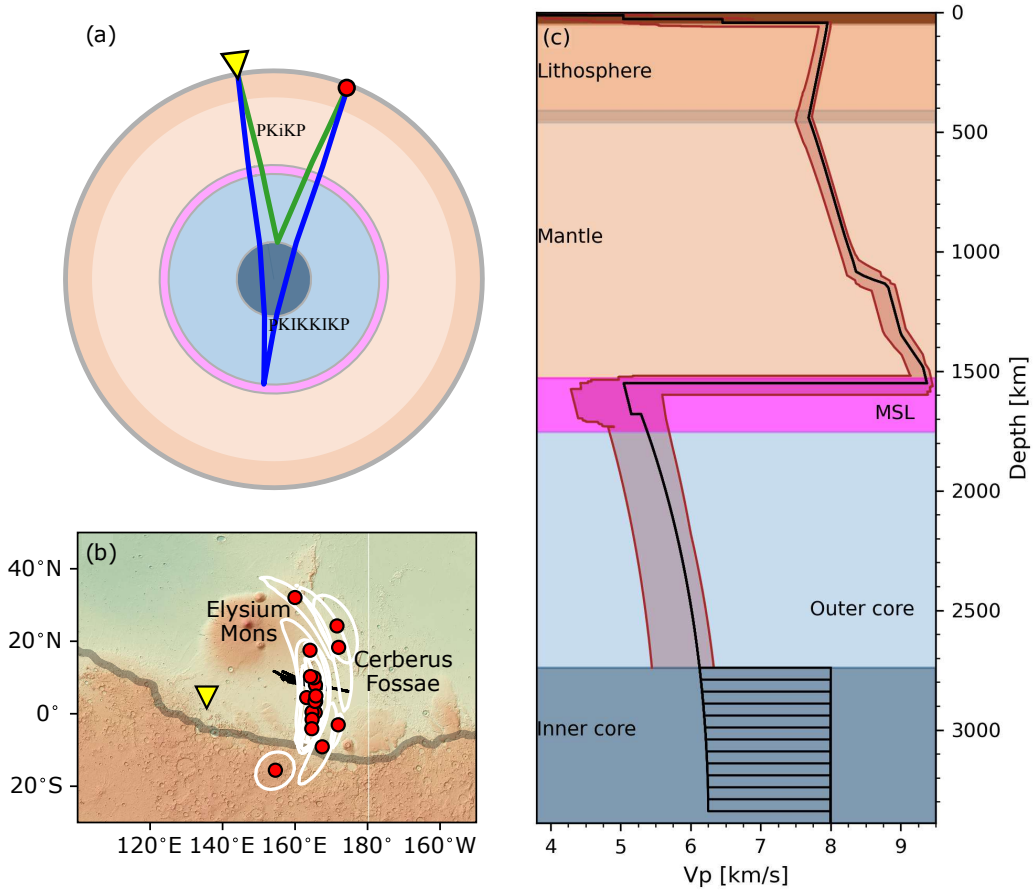


Figure 1. Overview of location of marsquakes and interior models used in this study. (a) Inner-core body wave ray paths, showing top-side inner-core reflection (PKiKP) and bottom-side outer-core reflection (PKIKKIKP). (b) Distribution of events in Cerberus Fossae (filled red circles) and uncertainty ellipses (white lines). InSight is indicated by the inverted yellow triangle. (c) Interior structure models of Mars (from Khan et al., 2023). MSL indicates the molten silicate layer. Note that inner-core P-wave velocity (V_P) is unconstrained in these models. The solid black line represents the reference model.

To apply the source stacking procedure, we predict for each event travel times for the phase of interest using `TauP` (Crotwell et al., 1999; Crotwell, 2025) and a representative radial martian seismic velocity profile in the form of the mean model from Khan et al. (2023). As illustrated in Figure 1, we vary the radius of the inner core in this model between 50 and 650 km in 50-km increments, and repeat the travel time calculation for each model. Since we are only interested in the reflection from the inner-core boundary, P- and S-wave speeds and density in the inner core are fixed (to 8 km/s, 5 km/s and 7 g/cm^3).

The traces, now aligned on the phase of interest, are linearly stacked as:

$$b(t) = \frac{1}{N}\sum_{i=1}^{N} x_i(t - t_m), \tag{1}$$

where $b(t)$ is the resultant beam of traces, x_i is each trace in the source array of N traces, and t_m is the predicted arrival time for this phase. This method is largely analogous to the analysis proposed by Bi et al. (2025).

To further enhance the precision of the slowness measurement we calculate the F-vespagram, a measure of coherence (Selby, 2008; Frost et al., 2013). The coherence, F, is calculated as the ratio between the total squared energy within the beam, $b(t)$, and the total squared differences between the beam and each trace used to form the beam $x_i(t)$, calculated in a 2 s moving time window and normalized by the number of traces in the beam, N:

$$F(t) = \frac{(N-1)}{N} \frac{\sum_{t_j=t-1\ \mathrm{s}}^{t+1\ \mathrm{s}} b(t_j)^2}{\sum_{i=1}^{N} \sum_{t_j=t-1\ \mathrm{s}}^{t+1\ \mathrm{s}} \left(x_i(t_j) - b(t_j)\right)^2} \tag{2}$$

The radial reference model (Figure 1) used is our best estimate of the velocity structure of Mars, but likely is not the true velocity structure. To account for this, we apply a correction to the predicted time t_m depending on the distance of each event from the reference distance and the horizontal slowness, u_{hor}, the inverse of the apparent horizontal seismic velocity at the surface, v_{app}. We perform a grid-search over relative u_{hor} in a range of ± 4 s/km with increments of 0.02 s/km relative to the predicted slowness for the phase of interest. We recompute the beam and F-trace at each relative slowness and use these to form vespagrams and F-vespagrams, respectively. We identify the phase as the peak coherence in the vespagram and F-vespagrams within the expected time and slowness windows for each inner core radius, accounting for mantle variability across the velocity models of Khan et al. (2023) shown in Figure 1 and uncertainties in the epicentral distance of the events (Table S1).

In the search for a particular phase, such as the inner-core reflection, we look for the model producing the highest coherence and beam-amplitude (for a given inner-core radius). The model with the highest coherence and beam-amplitude is the one for which alignment is optimal and the traces in the source array therefore sums most coherently. For robustness, we also require that the peak coherence in the vespagram and F-vespagram are similar.

The method is applicable to any body wave phase, such as SS, PP, SSS, PPP, ScS, PKiKP and PKIKKIKP. To illustrate the methodology, we first consider the phases, which have been seen by other means by the InSight team (e.g., Durán et al., 2022). Following this, we focus on inner-core phases.

3 Results and Discussion

3.1 Application to established body waves

To test our method, we verified it on a previously seen phase, the surface reflection (SS). The results are summarised in Figure 2. The slownesses based on the peak values in the vespagram and F-vespagram are similar, resulting in coherent waveform alignment and stacked waveforms showing prominent arrivals about ∼20 s after the main S-wave arrival, in good agreement with earlier observations of the SS-wave from Cerberus Fossae marsquakes (e.g., Durán et al., 2022; Drilleau et al., 2022).

We extended the analysis to include the other body wave phases seen by the InSight team, notably PP (Figure S1), PPP (Figure S2), SSS (Figure S3) and ScS, which, strictly speaking, should be referred to as SdS given that it is a reflection from the top of the molten layer and not the core (Figure S4). In the case of ScS/SdS, we find a solid mantle–molten silicate layer boundary between 1820–1900 km, which is in good agree-

ment with earlier studies, where the same boundary was determined to be in the range 1770–1890 km (e.g., Stähler et al., 2021; Durán et al., 2022; Drilleau et al., 2022; Irving et al., 2023; Le Maistre et al., 2023; Wang & Tkalčić, 2022; Khan et al., 2023; Samuel et al., 2023).

3.2 Application to PKiKP

We grid-searched over a range of inner core models with radii between 50 and 650 km in increments of 50 km (Figure 1), accounting, as before, for mantle variability across the velocity models of Khan et al. (2023) and uncertainties in the epicentral distance of the events. The results based on the F-vespagrams are shown in Figure 3 (vespagrams and corresponding stacked waveforms are shown in Figure S5) and indicate, in addition to the 600-km inner-core model of Bi et al. (2025), maximum beam amplitudes and coherence for a range of inner-core models with core radii of 200, 300, 500 km (note that beam amplitudes for inner-core radii of 200 and 300 km are actually larger than those for the 600-km model). Because the peak coherence in the vespagram and F-vespagram for a 400-km inner-core are dissimilar, this particular model is not considered robust. Similar plots at 50-km intervals are shown in Figures S6–S7 and indicate that similar maximum beam amplitude and coherence signals are also obtained for a range of inner-core radii between 200–300 km and 500–600 km. Except for the additional diagnostic, the F-vespagram, our analysis aligns with the approach taken by Bi et al. (2025); however, Bi et al. (2025) only stacked data for an inner core with a fixed radius of 600 km, whereas we considered a range of inner-core radii from 100 to 600 km.

3.3 Application to PKIKKIKP

As for PKiKP, we grid-searched over inner-core models with radii between 50 and 650 km in increments of 50 km (Figure 1), considering, as before, mantle velocity variability and uncertainties in the epicentral distance of the events. To account for unknown inner-core seismic properties, we additionally varied P-wave velocity between 7–8 km/s (Bi et al. (2025) consider 7–9 km/s), keeping S-wave velocity and density fixed, since PKIKKIKP is insensitive to the latter parameters. The results based on the F-vespagrams are shown in Figure 4 and, as in the case of PKiKP, we find maximum beam amplitudes and coherence for a range of inner-core models with radii ranging from 100 to 600 km. The time windows for PKIKKIKP, relative to PKiKP, increase from ∼60 s to ∼90 s, further confirming the aforementioned observation that phases traversing the inner core provide less definitive constraints. Similar results are obtained for an inner-core P-wave velocity of 7 km/s, as shown in Figure S8.

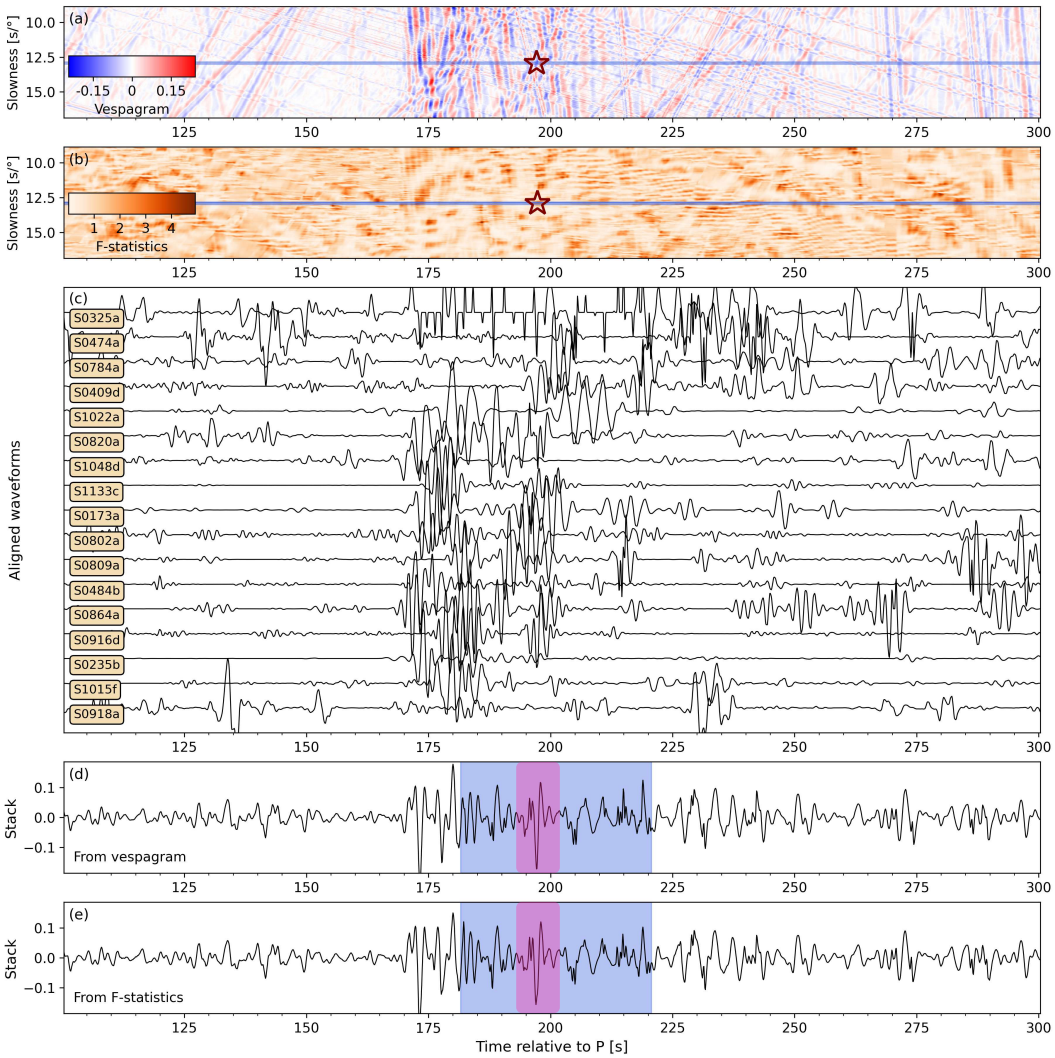


Figure 2. Summary of vespagram and F-vespagram analysis applied to the surface reflection body wave phase SS. (a) Vespagram; (b) F-vespagram; (c) normalized waveforms aligned based on slowness picked on the vespagram; (d) stacked waveforms based on vespagram; and (e) stacked waveforms based on F-vespagram. Red stars on panels (a) and (b) denote the picked slownesses used to generate the waveform stacks in panels (d) and (e), respectively. Times are relative to the predicted P-wave arrival for the reference distance (31°) and velocity model (mean model shown in figure 1). The light blue horizontal (a,b) and vertical (d,e) bars indicate the expected SS slowness and arrival time windows, respectively, for the mantle models of Khan et al. (2023), including uncertainties in event distances. Magenta-shaded windows indicate seismic arrivals consistent with SS-wave arrival.

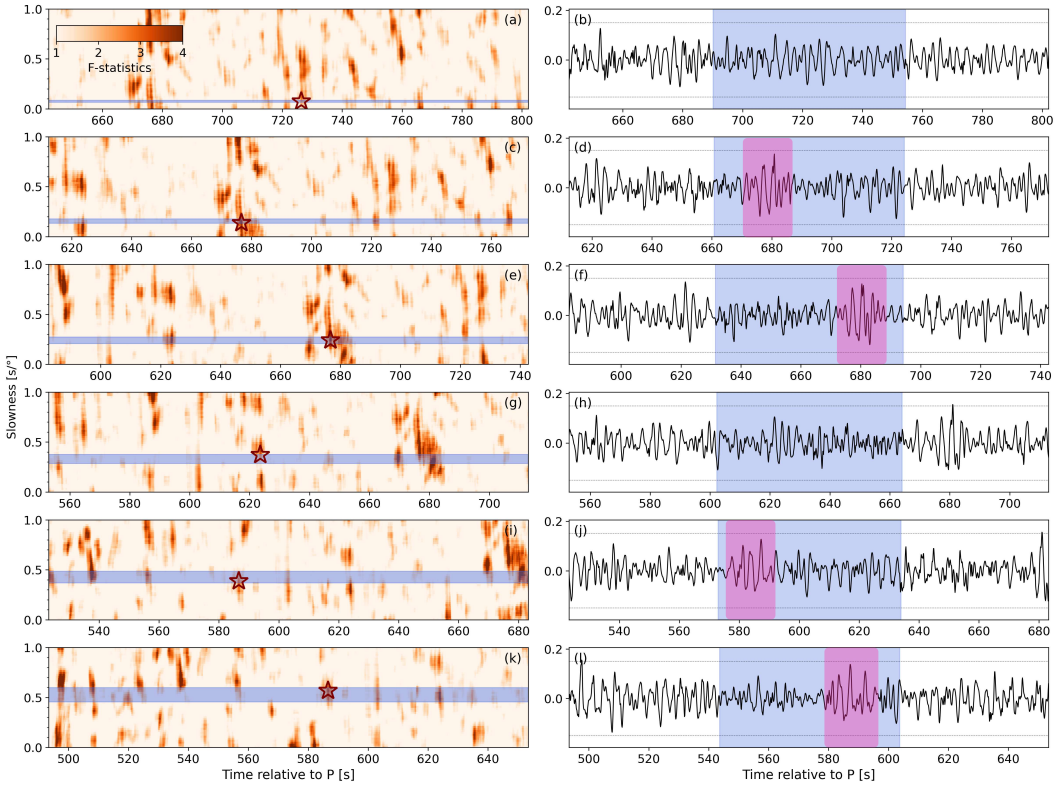


Figure 3. PKiKP F-vespagrams (left) and corresponding stacked waveforms (right) computed for 23 marsquakes with epicentral distances in the range 30°–40° (Table S1), assuming hypothetical inner core radii of (a-b) 100 km; (c-d) 200 km; (e-f) 300 km; (g-h) 400 km; (i-j) 500 km; and (k-l) 600 km. On each vespagram, the red star denotes the picked slowness used to generate the waveform stack (righthand panels). Times are relative to the predicted P-wave arrival for the reference distance (31°) and velocity model (shown in figure 1). The light blue shading highlights the expected PKiKP slowness window (horizontal blue bars, lefthand panels) and arrival time window (vertical blue bars, righthand panels) for each inner core radius, accounting for mantle variability across the velocity models of Khan et al. (2023) and uncertainties in the epicentral distance of the events. Light magenta shaded windows highlight observed seismic arrivals consistent with potential inner core reflections. A similar version for inner-core radii sampled at 50-km intervals is available in the supplementary information (Figure S7).

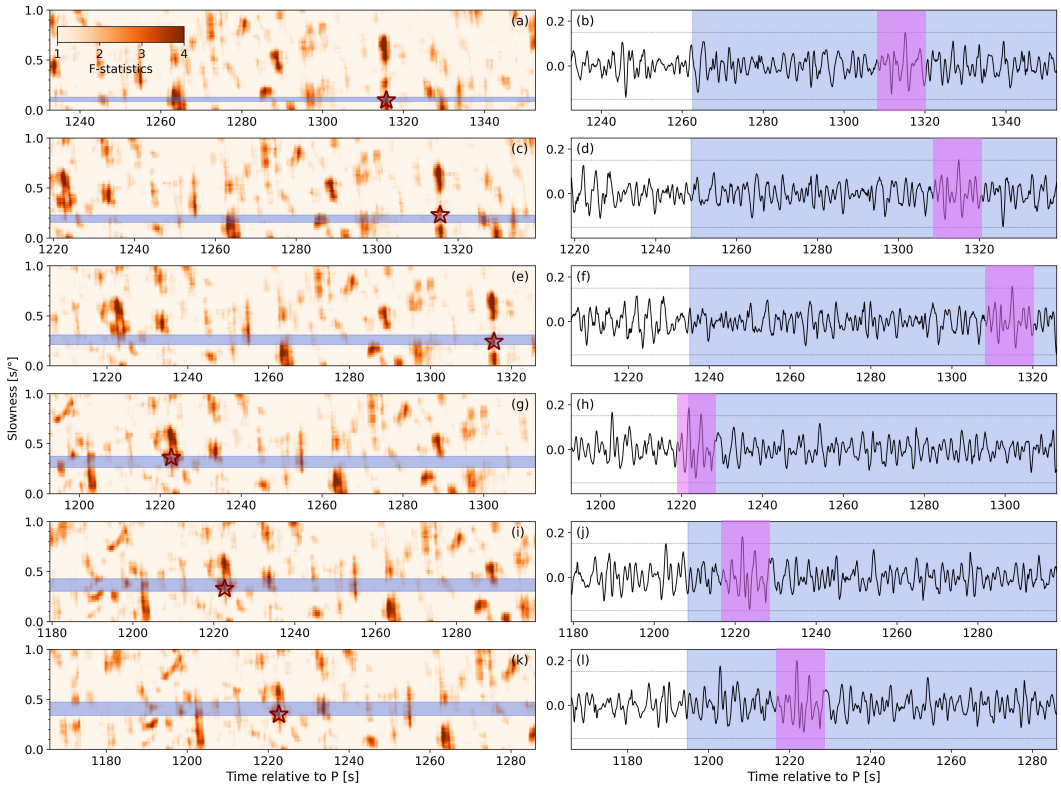


Figure 4. PKIKKIKP F-vespagram (left) and corresponding stacked waveforms (right) computed for 23 marsquakes with epicentral distances in the range 30°–40° (Table S1), assuming hypothetical inner core radii of (a-b) 100 km; (c-d) 200 km; (e-f) 300 km; (g-h) 400 km; (i-j) 500 km; and (k-l) 600 km. Inner-core P-wave velocity is assumed to be 8 km/s. On each F-vespagram, the red star denotes the picked slowness used to generate the waveform stack (right-hand panels). Times are relative to the predicted P-wave arrival for the reference distance (31°) and velocity model (shown in figure 1 in the main manuscript). The light blue shading highlights the expected PKIKKIKP slowness window (horizontal blue bars, lefthand panels) and arrival time window (vertical blue bars, righthand panels) for each inner core radius, accounting for mantle variability across the velocity models of Khan et al. (2023) and uncertainties in the epicentral distance of the events. Light magenta shaded windows highlight observed wave packets consistent with potential PKIKKIKP arrivals.

4 Summary and Conclusion

Motivated by a recent study proposing the presence of an inner-core on Mars (Bi et al., 2025), we reanalysed the same seismic data from the Mars InSight mission to search for reflections from the inner-core boundary (PKiKP) and reflections from the inside of the liquid outer core (PKIKKIKP) that were also considered by Bi et al. (2025). Using source-array stacking to enhance the signal-to-noise ratio of these weak arrivals, we confirm most of the body-wave phases (e.g., PP, SS, PPP, SSS, and ScS) previously identified using independent techniques (waveform matching, polarisation analysis, and filterbanks). However, when applying the same method to the inner-core signals, we find that these phases produce coherent signals for multiple candidate inner-core radius ranges for PKiKP (200–300 km and 500–600 km) and for PKIKKIKP (100–600 km). The range for the latter phase is larger because of the additional uncertainty associated with the unknown inner-core P-wave velocity. The results for all investigated phases using source-array analysis are summarised in Table 1.

Ultimately, the results indicate that the PKiKP and PKIKKIKP observations are consistent with multiple inner-core models and therefore do not constitute conclusive evidence for the existence of an inner core on Mars.

Table 1. Summary of body wave phases seen through source-array analysis. Phases are classified as either identified ("✓"), possibly identified ("(✓)") or not conclusively identified ("×"). Phases marked as possibly identified are those for which the peak coherency in the vespagram and F-vespagram do not coincide.

Phase	Identified
SS	✓
SSS	(✓)
PP	✓
PPP	✓
SdS	✓
PKiKP	×
PKIKKIKP	×

Open Research

Waveforms and codes are available upon request.

Acknowledgments

We acknowledge NASA, CNES, partner agencies and institutions (UKSA, SSO, DLR, JPL, IPGP-CNRS, ETHZ, ICL, MPS-MPG), and the operators of JPL, SISMOC, MSDS, IRIS-DMC and PDS for providing SEED SEIS data. We would like to thank Savas Ceylan for help with Figure 1. This work was supported by a grant from the Swiss National Science Foundation (Project 10003243).

References

Banerdt, W. B., Smrekar, S. E., Banfield, D., Giardini, D., Golombek, M., Johnson, C. L., ... Wieczorek, M. (2020). Initial results from the InSight mission on Mars.

Nature Geoscience, *13*(3), 183-189. doi: 10.1038/s41561-020-0544-y

Bi, H., Sun, D., Sun, N., Mao, Z., Dai, M., & Hemingway, D. (2025). Seismic detection of a 600-km solid inner core in Mars. , *645*(8079), 67-72. doi: 10.1038/s41586-025-09361-9

Brinkman, N., Stähler, S. C., Giardini, D., Schmelzbach, C., Khan, A., Jacob, A., ... Banerdt, W. B. (2021). First focal mechanisms of marsquakes. *Journal of Geophysical Research: Planets*, *126*(4), e2020JE006546. (e2020JE006546 2020JE006546) doi: 10.1029/2020JE006546

Buono, A. S., & Walker, D. (2011). The fe-rich liquidus in the fe–fes system from 1bar to 10gpa. *Geochimica et Cosmochimica Acta*, *75*(8), 2072-2087. doi: 10.1016/j.gca.2011.01.030

Crotwell, H. P. (2025). *The tauP Toolkit*. Zenodo. doi: 10.5281/zenodo.10794858

Crotwell, H. P., Owens, T. J., & Ritsema, J. (1999). The taup toolkit: Flexible seismic travel-time and ray-path utilities. *Seismological Research Letters*, *70*(2), 154–160. doi: 10.1785/gssrl.70.2.154

Drilleau, M., Samuel, H., Garcia, R. F., Rivoldini, A., Perrin, C., Michaut, C., ... Banerdt, W. B. (2022). Marsquake Locations and 1-D Seismic Models for Mars From InSight Data. *Journal of Geophysical Research (Planets)*, *127*(9), e07067. doi: 10.1029/2021JE007067

Durán, C., Khan, A., Ceylan, S., Zenhäusern, G., Stähler, S., Clinton, J. F., & Giardini, D. (2022). Seismology on Mars: An analysis of direct, reflected, and converted seismic body waves with implications for interior structure. *Physics of the Earth and Planetary Interiors*, *325*, 106851. doi: 10.1016/j.pepi.2022.106851

Durán, C., Khan, A., Ceylan, S., Charalambous, C., Kim, D., Drilleau, M., ... Giardini, D. (2022). Observation of a Core-Diffracted P-Wave From a Farside Impact With Implications for the Lower-Mantle Structure of Mars. *Geophysical Research Letters*, *49*(21), e2022GL100887. doi: 10.1029/2022GL100887

Frost, D. A., Rost, S., Selby, N. D., & Stuart, G. W. (2013). Detection of a tall ridge at the core–mantle boundary from scattered PKP energy. *Geophysical Journal International*, *195*(1), 558–574.

InSight Marsquake Service. (2023). *Mars seismic catalogue, insight mission; v14 2023-04-01*. ETHZ, IPGP, JPL, ICL, Univ. Bristol. Retrieved from `https://www.insight.ethz.ch/seismicity/catalog/v14` doi: 10.12686/a21

Irving, J. C. E., Lekić, V., Durán, C., Drilleau, M., Kim, D., Rivoldini, A., ... Xu, Z. (2023). First observations of core-transiting seismic phases on Mars. *Proceedings of the National Academy of Science*, *120*(18), e2217090120. doi: 10.1073/pnas.2217090120

Jacob, A., Plasman, M., Perrin, C., Fuji, N., Lognonné, P., Xu, Z., ... Banerdt, W. (2022). Seismic sources of insight marsquakes and seismotectonic context of elysium planitia, mars. *Tectonophysics*, *837*, 229434. doi: 10.1016/j.tecto.2022.229434

Khan, A., Huang, D., Durán, C., Sossi, P. A., Giardini, D., & Murakami, M. (2023). Evidence for a liquid silicate layer atop the Martian core. *Nature*, *622*(7984), 718-723. doi: 10.1038/s41586-023-06586-4

Khan, A., Sossi, P. A., Liebske, C., Rivoldini, A., & Giardini, D. (2022). Geophysical and cosmochemical evidence for a volatile-rich Mars. *Earth and Planetary Science Letters*, *578*, 117330. doi: 10.1016/j.epsl.2021.117330

Komabayashi, T., Thompson, S., & Robertson, M. (2026). Sulfur in the cores of the earth, mars, and the moon. In D. E. Harlov & G. S. Pokrovski (Eds.), *The role of sulfur in planetary processes: From cores to atmospheres* (pp. 1013–1057). Cham: Springer Nature Switzerland. doi: 10.1007/978-3-032-07705-9_14

Le Maistre, S., Rivoldini, A., Caldiero, A., Yseboodt, M., Baland, R.-M., Beuthe, M., ... Banerdt, W. B. (2023, July). Spin state and deep interior structure of Mars from InSight radio tracking. *Nature*, *619*(7971), 733-737. doi:

10.1038/s41586-023-06150-0

Lognonné, P., Banerdt, W. B., Clinton, J., Garcia, R. F., Giardini, D., Knapmeyer-Endrun, B., ... Pike, W. T. (2023, May). Mars Seismology. *Annual Review of Earth and Planetary Sciences*, *51*, 643-670. doi: 10.1146/annurev-earth-031621-073318

Mittelholz, A., Johnson, C. L., Thorne, S. N., Joy, S., Barrett, E., Fillingim, M. O., ... Banerdt, W. B. (2020). The origin of observed magnetic variability for a sol on mars from insight. *Journal of Geophysical Research: Planets*, *125*(9), e2020JE006505. doi: 10.1029/2020JE006505

Montalbetti, J. F., & Kanasewich, E. R. (1970). Enhancement of teleseismic body phases with a polarization filter. *Geophysical Journal International*, *21*(2), 119–129.

Niazi, M. (1969). Use of source arrays in studies of regional structure. *Bulletin of the Seismological Society of America*, *59*(4), 1631–1643.

Perrin, C., Jacob, A., Lucas, A., Myhill, R., Hauber, E., Batov, A., ... Fuji, N. (2022). Geometry and segmentation of cerberus fossae, mars: Implications for marsquake properties. *Journal of Geophysical Research: Planets*, *127*(1), e2021JE007118. (e2021JE007118 2021JE007118) doi: 10.1029/2021JE007118

Posiolova, L. V., Lognonné, P., Banerdt, W. B., Clinton, J., Collins, G. S., Kawamura, T., ... Zenhäusern, G. (2022). Largest recent impact craters on mars: Orbital imaging and surface seismic co-investigation. *Science*, *378*(6618), 412-417. doi: 10.1126/science.abq7704

Rost, S., & Thomas, C. (2002). Array seismology: Methods and applications. *Reviews of Geophysics*, *40*(3), 2-1-2-27. doi: 10.1029/2000RG000100

Rost, S., & Thomas, C. (2009). Improving seismic resolution through array processing techniques. *Surveys in geophysics*, *30*(4), 271–299.

Samuel, H., Drilleau, M., Rivoldini, A., Xu, Z., Huang, Q., Garcia, R. F., ... Banerdt, W. B. (2023). Geophysical evidence for an enriched molten silicate layer above Mars's core. *Nature*, *622*(7984), 712-717. doi: 10.1038/s41586-023-06601-8

Scherbaum, F., Gillard, D., & Deichmann, N. (1991). Slowness power spectrum analysis of the coda composition of two microearthquake clusters in northern Switzerland. *Physics of the earth and planetary interiors*, *67*(1-2), 137–161.

Selby, N. D. (2008). Application of a generalized F detector at a seismometer array. *Bulletin of the Seismological Society of America*, *98*(5), 2469–2481.

Spudich, P., & Bostwick, T. (1987). Studies of the seismic coda using an earthquake cluster as a deeply buried seismograph array. *Journal of Geophysical Research: Solid Earth*, *92*(B10), 10526–10546.

Stähler, S. C., Khan, A., Banerdt, W. B., Lognonné, P., Giardini, D., Ceylan, S., ... Smrekar, S. E. (2021). Seismic detection of the martian core. *Science*, *373*(6553), 443-448. doi: 10.1126/science.abi7730

Stähler, S. C., Mittelholz, A., Perrin, C., Kawamura, T., Kim, D., Knapmeyer, M., ... others (2022). Tectonics of Cerberus Fossae unveiled by marsquakes. *Nature Astronomy*, 1–11. doi: 0.1038/s41550-022-01803-y

Stevenson, D. J. (2001). Mars' core and magnetism. *Nature*, *412*, 214-219.

Thomas, C., Heyn, B. H., Tölle, L., & van Tent, R. (2025, Jul.). Investigating the d" reflector beneath the indian ocean with source arrays. *Seismica*, *4*(2). doi: 10.26443/seismica.v4i2.1418

Wang, S., & Tkalčić, H. (2022). Scanning for planetary cores with single-receiver intersource correlations. *Nature Astronomy*, *6*(11), 1272–1279. doi: 10.1038/s41550-022-01796-8

Yan, C., Barik, A., Stanley, S., Mittelholz, A., Plesa, A.-C., & Johnson, C.-L. (2025). Mars' hemispheric magnetic field from a full-sphere dynamo. *Geophysical Research Letters*, *52*(3), e2024GL113926. (e2024GL113926 2024GL113926) doi: 10.1029/2024GL113926

Supplementary Files

This is a list of supplementary files associated with this preprint. Click to download.

- VisseretalSM.pdf